Safety Studies in Tumor and Non-Tumor-Bearing Mice in Support of Clinical Trials Using Oncolytic VSV-IFNβ-NIS

Lianwen Zhang,[1] Michael B. Steele,[1,2] Nathan Jenks,[1,2] Jacquelyn Grell,[1,2] Lukkana Suksanpaisan,[3] Shruthi Naik,[1] Mark J. Federspiel,[1,4] Martha Q. Lacy,[5] Stephen J. Russell,[1,5] and Kah-Whye Peng[1,2,*]

[1]Department of Molecular Medicine, Mayo Clinic, Rochester, Minnesota; [2]Toxicology and Pharmacology Laboratory, Mayo Clinic, Rochester, Minnesota; [3]Imanis Life Sciences, Rochester, Minnesota; [4]Viral Vector Production Laboratory, Mayo Clinic, Rochester, Minnesota; and [5]Division of Hematology, Mayo Clinic, Rochester, Minnesota

Oncolytic VSV-IFNβ-NIS is selectively destructive to tumors. Here, we present the IND enabling preclinical rodent studies in support of clinical testing of vesicular stomatitis virus (VSV) as a systemic therapy. Efficacy studies showed dose-dependent tumor regression in C57BL/KaLwRij mice bearing syngeneic 5TGM1 plasmacytomas after systemic VSV administration. In contrast, the virus was effective at all doses tested against human KAS6/1 xenografts in SCID mice. Intravenous administration of VSV-mIFNβ-NIS is well tolerated in C57BL/6 mice up to 5×10^{10} $TCID_{50}$ (50% tissue culture infective dose)/kg with no neurovirulence, no cytokine storm, and no abnormalities in tissues. Dose-limiting toxicities included elevated transaminases, thrombocytopenia, and lymphopenia. Inactivated viral particles did not cause hepatic toxicity. Intravenously administered VSV was preferentially sequestered by macrophages in the spleen and liver. Quantitative RT-PCR analysis for total viral RNA on days 2, 7, 21, and 58 showed highest VSV RNA in day 2 samples; highest in spleen, liver, lung, lymph node, kidney, gonad, and bone marrow. No infectious virus was recovered from tissues at any time point. The no observable adverse event level and maximum tolerated dose of VSV-mIFNβ-NIS in C57BL/6 mice are 10^{10} $TCID_{50}$/kg and 5×10^{10} $TCID_{50}$/kg, respectively. Clinical translation of VSV-IFNβ-NIS is underway in companion dogs with cancer and in human patients with relapsed hematological malignancies and endometrial cancer.

INTRODUCTION

THE INDIANA LABORATORY-adapted strain of vesicular stomatitis virus (VSV) has promising oncolytic activity and is being developed as an anticancer agent with enhanced safety and therapeutic usefulness.[1] VSV-IFNβ-NIS is a novel recombinant VSV genetically engineered to express the human sodium iodide symporter (NIS) as a reporter gene and human interferon (hIFN)-β to minimize viral replication in normal cells.[2] We previously showed that high doses of VSV encoding murine IFN-β (VSV-mIFNβ-NIS) induced complete remission of established 5TGM1 plasmacytomas in immunocompetent mice.[2] The virus extravasated from tumor blood vessels and rapidly infected surrounding tumor cells, forming multiple intratumoral infectious centers that expand rapidly, coalesce, and necrose at their centers.[3] In this permissive 5TGM1 model, the oncolytic tumor debulking phase is rapid and completed by 72 hr after virus administration. Immune-mediated clearance of residual tumor cells protected the mice from tumor challenge and is most effective in mice treated with VSV-mIFNβ-NIS, which encodes the biologically active murine IFNβ.[2,4] Using high-resolution NIS reporter gene imaging of tumors in each animal, we showed that anesthesia resulted in decreased intratumoral infection density, and that exercise increased the density and uniformity of infectious centers.[5] Indeed, mathematical modeling predicted that small changes to the density of initially infected cells or to the average maximum radius of infected centers would have a major impact on treatment outcome.[3]

Clinical testing of a recombinant VSV encoding the canine IFN-β and NIS (VSV-cIFNβ-NIS) is ongoing in a National Cancer Institute (NCI, Bethesda,

*Correspondence: Dr. Kah-Whye Peng, Department of Molecular Medicine, Mayo Clinic, 200 First Street SW, Rochester, MN 55905. E-mail: peng.kah@mayo.edu

DOI: 10.1089/humc.2016.061

MD)-coordinated comparative oncology study in companion dogs with cancer (study COTC-024). Safety studies in research beagles before the start of the canine trial indicated that the maximal tolerated dose (MTD) in dogs is 10^{10} $TCID_{50}$ (50% tissue culture infective dose) of VSV-hIFNβ-NIS or VSV-cIFNβ-NIS.[6] At $10\times$MTD (10^{11} $TCID_{50}$), the dose-limiting toxicity is severe hepatotoxicity with elevations in transaminases and prolongation of partial thromboplastin time (PTT), requiring euthanasia of the animal. Intensive pharmacokinetics studies showed a rapid increase in VSV-nucleocapsid (N) RNA in the blood from 10 min to 3 hr after virus infusion (end of acute-phase monitoring). Viral RNA is significantly diminished 24 hr after virus infusion and continues to decline over several days, and was undetectable by day 10. No infectious virus was recovered from the blood, urine, or buccal swabs taken at any time point. Anti-VSV antibodies were rapidly generated and readily detectable by day 5 after virus infusion.[6]

In support of our investigational new drug (IND) application to the U.S. Food and Drug Administration (FDA) for clinical testing of VSV-hIFNβ-NIS in humans with disseminated cancer, the Mayo Clinic Virus and Gene Therapy Toxicology and Pharmacology Laboratory performed prospectively designed biodistribution (BD) and safety studies in rodents, with input and guidance from the Pharmacology and Toxicology Branch of the Center for Biologics Evaluation and Research (CBER) of the FDA. Quality assurance (QA) of the in-life studies was performed by the Mayo Clinic Regulatory Compliance Unit, and the QA review of the final reports submitted in the IND package was performed by an independent external reviewer. In addition, we also performed research studies in mice to evaluate the mechanisms underlying the hepatotoxicity associated with high intravenous doses of VSV.

RESULTS

VSV-induced elevations in transaminases require live virus

Pilot studies revealed that liver enzymes were elevated at 24 hr with systemic administration of 10^9 $TCID_{50}$ of VSV-mIFNβ-NIS but not with lower (10^8 or 3×10^8) doses of virus into C57BL/6 mice. To determine whether transient transaminitis is due to the presence of large amounts of viral particles, 10^9 $TCID_{50}$ of infectious virus or equivalent amounts of heat-inactivated VSV-mIFNβ-NIS were given intravenously to mice. In mice given infectious VSV, both aspartate transaminase (AST) and alanine transaminase (ALT) levels were significantly elevated at 24 hr ($p=0.002$ for ALT, $p=0.005$ for AST), coupled with a significant decrease in platelets and lymphocytes at 24 hr (Fig. 1a–c). In contrast, inactivated VSV particles induced only a small increase in AST at 3 hr and returned to normal by 24 hr, confirming that active viral infection was required for significant elevation of transaminase levels (Fig. 1a–c). Importantly, transaminitis was transient and enzyme levels returned to baseline levels by 48 hr.

VSV is sequestered by cells of the reticuloendothelial system

To determine the cell types that were infected with VSV, we injected C57BL/6 mice intravenously with 3×10^8 $TCID_{50}$ of DiI (1,1′-dioctadecyl-3,3,3′,3′-tetramethylindocarbocyanine perchlorate)-labeled VSV and found abundant red fluorescent cells in the liver and spleen, which had sequestered the labeled virus (Fig. 1d). Immunohistochemical staining for the macrophage marker CD68 (green) at 3 hr showed clear colocalization of red DiI-labeled cells and $CD68^+$ (green) macrophages, revealing that VSV virions were preferentially sequestered by macrophages in the spleen (Fig. 1e) and liver (data not shown). Quantitative RT-PCR analysis showed high levels of VSV-N RNA (viral mRNA and genomes) at 3 hr (limit of detection is >1000 copies/μg cellular RNA). VSV-N RNA declined steadily over 24 and 48 hr in liver and spleen (Fig. 1f). Infectious virus was not detectable in the liver (limit of detection is >190 $TCID_{50}$/ml), but a low level of infectious VSV (10^4 $TCID_{50}$/g tissue) was recovered from the spleen only at 24 hr (Fig. 1g). In contrast, no live virus was recovered from tissues of mice given inactivated VSV.

We previously reported that murine IFN-β, between 2 and 4 ng/ml, is detected in the serum of 5TGM1 tumor-bearing mice treated with VSV-mIFN-NIS.[2] A multiplex cytokine assay that measures interleukin (IL)-1β, IL-10, IL-6, IL-12, granulocyte-macrophage colony-stimulating factor (GM-CSF), IL-5, IFN-γ, tumor necrosis factor (TNF)-α, IL-2, and IL-4 was performed on plasma collected at 3 and 24 hr from C57BL/6 mice given 10^8, 3×10^8, or 10^9 $TCID_{50}$ of VSV-mIFNβ-NIS (Table 1, $n=5$ mice per time point). The change in levels of inflammatory cytokines, TNF-α, IFN-γ, and IL-12 was unremarkable between the three VSV dose levels or when compared with the saline controls. The only appreciable increase was of IL-6, from <5 pg/ml in saline controls to 125 pg/ml at 24 hr in the 10^9 $TCID_{50}$ group. In summary, no cytokine storm is evident in VSV-treated animals at doses ranging from 10^8 to 10^9 $TCID_{50}$.

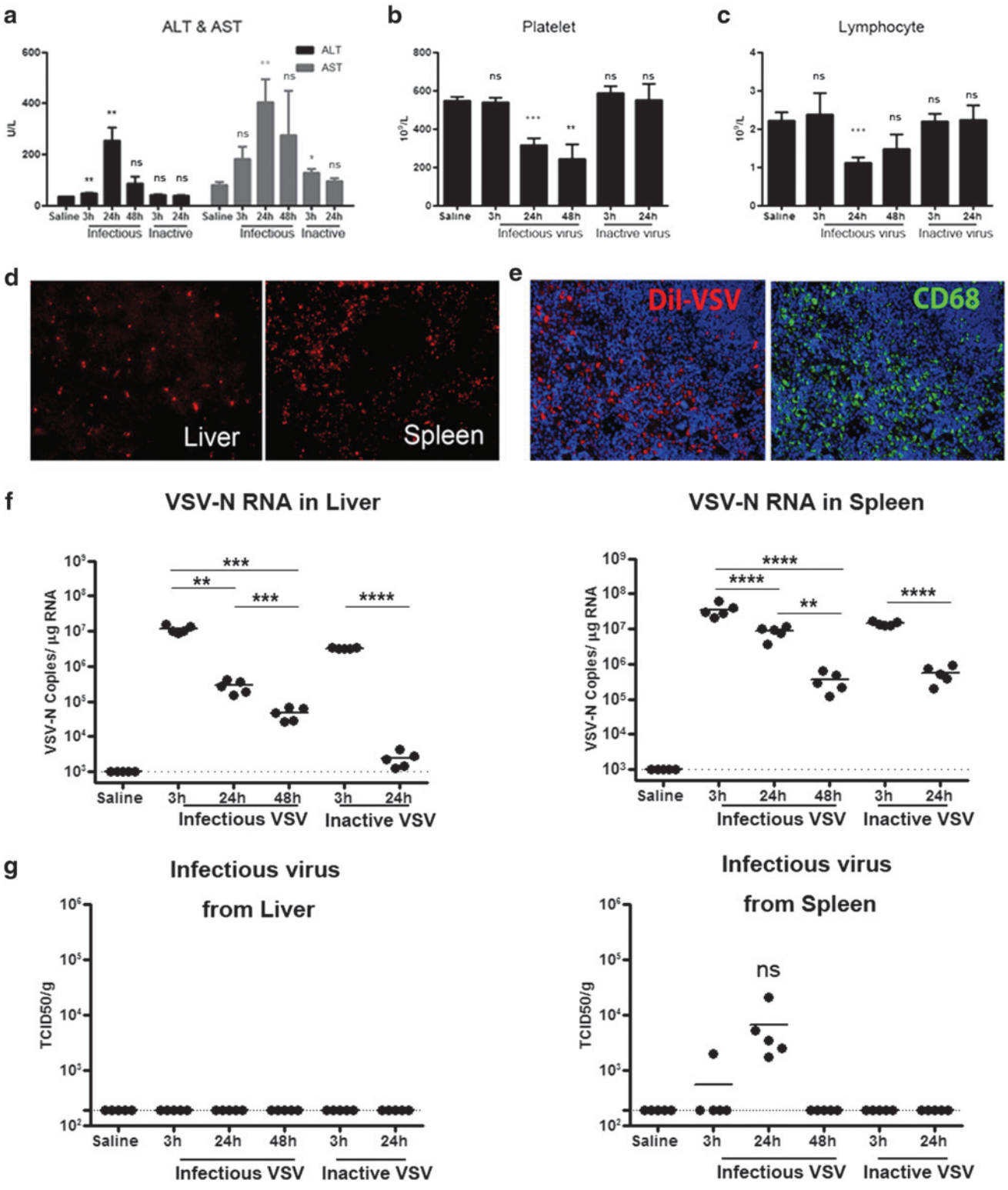

Figure 1. Systemic administration of 10^9 $TCID_{50}$ (50% tissue culture infective dose) of infectious but not inactive VSV-mIFNβ-NIS is associated with acute but transient hepatic toxicity, thrombocytopenia, and lymphopenia in C57BL/6 mice. **(a)** Alanine transaminase (ALT) and aspartate transaminase (AST) levels increased significantly at 3 and 24 hr but returned to baseline by 48 hr. **(b)** Platelet and **(c)** lymphocyte counts were decreased by 24 hr in VSV-treated mice. Significance was determined by comparison with saline controls. **(d)** Sequestration of DiI-labeled VSV by cells in the liver and spleen. **(e)** Spleen section showing good colocalization of red DiI-positive cells with CD68 staining (green). **(f** and **g)** qRT-PCR for VSV-N (nucleocapsid) RNA **(f)** and infectious virus recovery in liver and spleen **(g)**. *$p \leq 0.05$, **$p \leq 0.01$, and ***$p \leq 0.001$; ns, not significant. Dotted line represents limits of detection: 190 $TCID_{50}$/g for infectious virus recovery (IVR), 10^3 copies/μg RNA for qRT-PCR.

Table 1. *Multiplex cytokine assay of plasma from mice 3 or 24 hours after intravenous VSV-mIFNβ-NIS virus administration*

Dose ($TCID_{50}$)	Time point (hr)	IL-1β (pg/ml)	IL-10 (pg/ml)	IL-6 (pg/ml)	IL-12 (pg/ml)	GM-CSF (pg/ml)	IL-5 (pg/ml)	IFN-γ (pg/ml)	TNF-α (pg/ml)	IL-2 (pg/ml)	IL-4 (pg/ml)
Saline	24	<5	<10	<5	96.6 ± 24	1.4 ± 0.7	19.1	<5	9.8 ± 3.5	<5	<20
VSV (1×10^8)	3	<5	<10	50.7 ± 30.5	83.4 ± 45.2	1.5 ± 0.6	23.9 ± 35.5	<5	24.5 ± 13.4	<5	<20
	24	<5	<10	<5	93.1 ± 85.2	1.7 ± 0.6	6.5 ± 12.0	<5	17.5 ± 15.9	<5	<20
VSV (3×10^8)	3	12.0 ± 8.4	<10	<5	114.9 ± 25.6	3.3 ± 1.3	11.9 ± 8.7	<5	54.9 ± 45.2	8.5 ± 5.2	<20
	24	10.1 ± 5.7	<10	<5	134.6 ± 33.8	1.7 ± 0.6	2.1 ± 2.3	<5	23.7 ± 17.7	<5	<20
VSV (1×10^9)	3	8.2 ± 6.0	<10	28.5 ± 26.8	92.3 ± 39.1	2.7 ± 0.8	7.1 ± 8.0	<5	25.3 ± 13.2	6 ± 0.5	<20
	24	16.5 ± 10.2	<10	125.2 ± 9.9	137.2 ± 30.3	4.5 ± 2.5	62.3 ± 48.7	<5	51.8 ± 31.7	10.9 ± 5.0	<20

GM-CSF, granulocyte-macrophage colony-stimulating factor; IFN, interferon; IL, interleukin; $TCID_{50}$, 50% tissue culture infective dose; TNF, tumor necrosis factor; VSV, vesicular stomatitis virus.

Depletion of macrophages by clodronate exacerbates VSV hepatotoxicity

Adenoviral particle-induced hepatotoxicity is associated with release of cytokines (and subsequent damage of hepatocytes) from activated macrophages that had sequestered intravenously administered viral particles.[7,8] To -understand the role of macrophages in VSV-induced hepatotoxicity, mice were treated intravenously with clodronate-loaded liposomes to deplete macrophages of the reticuloendothelial system. Two days after receiving clodronate or phosphate-buffered saline (PBS)-loaded liposomes, mice received 3×10^8 $TCID_{50}$ of VSV-mIFNβ-NIS. This lower viral dose was given, as 10^9 $TCID_{50}$ VSV was lethal in clodronate-treated mice (data not shown). In clodronate-treated mice, VSV induced a profound increase in ALT and AST (Fig. 2a). Quantitative RT-PCR analysis for VSV-N showed high levels of VSV-N in the liver and blood of clodronate-treated animals, although it was not significantly different from the nonclodronate/VSV animals ($p = 0.07$ for blood, and $p = 0.08$ for liver) (Fig. 2b and c). Low levels of infectious VSV were recovered from the livers of clodronate-treated mice depleted of macrophages (Fig. 2d).

Safety and biodistribution of VSV-mIFNβ-NIS in C57BL/6 mice

We next embarked on the IND enabling studies in support of systemic use of VSV-hIFNβ-NIS in

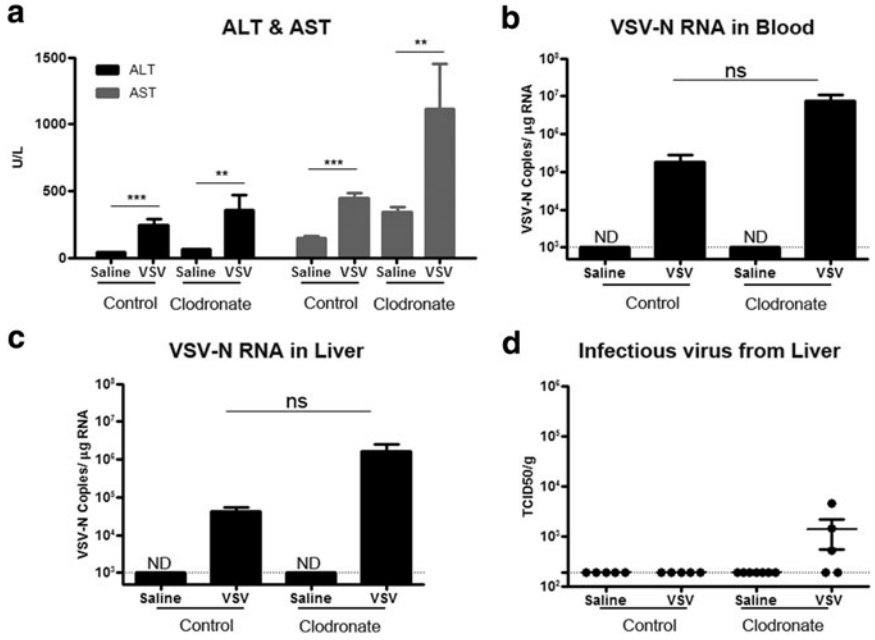

Figure 2. Depletion of macrophages by clodronate liposomes increased hepatic toxicity and VSV viral load in liver. C57BL/6 mice treated 2 days previously with saline or clodronate-loaded liposomes received 3×10^8 $TCID_{50}$ of VSV-mIFNβ-NIS intravenously. **(a)** ALT and AST levels, **(b)** VSV-N RNA in blood, **(c)** VSV-N RNA in liver, and **(d)** infectious virus recovered from liver. $^{**}p \le 0.01$, $^{***}p \le 0.001$; ND, not detectable; ns, not significant. Dotted line represents limits of detection: 10^3 copies/μg RNA for qRT-PCR and 190 $TCID_{50}$/g tissue for infectious virus recovery.

patients with end-stage cancer. Because human IFN-β has minimal biological activity in rodents, all rodent studies were performed with a VSV encoding murine IFN-β. The C57BL/6 mouse (6–7 weeks old) is permissive to VSV replication and is used as the model to evaluate potential toxicity and biodistribution of VSV at early (day 2), interim (days 7 and 21), and long-term (day 58) time points after intravenous administration. All groups included five mice of each sex. Each time point harvest consisted of 40 mice (5 males and five females per group); test articles included saline, VSV-mIFNβ-NIS at 10^8 $TCID_{50}$/mouse ($\sim 5\times10^9$ $TCID_{50}$/kg), 5×10^8 $TCID_{50}$/mouse ($\sim 1.5\times10^{10}$ $TCID_{50}$/kg), and 10^9 $TCID_{50}$/mouse ($\sim 5\times10^{10}$ $TCID_{50}$/kg). Overall, no dose-limiting toxicities or adverse events were observed in any treatment groups at any time point. There was a transient decrease in body weight immediately after dosing of test article (5–10% decline in VSV-treated mice, and 2% in saline-treated mice, on days 2–3) but increased thereafter (Fig. 3a).

Differences in complete blood count (CBC) and chemistries between treatment groups were analyzed by one-way analysis of variance (ANOVA) on day 2. There was a trend for decreased platelet counts in the virus-treated animals as the dose of VSV increased, although ANOVA showed no significant difference ($p=0.0514$) between the treatment groups (Fig. 3b). Similarly, there was a trend for decrease in lymphocytes, but it was not significant ($p=0.155$; Fig. 3c). There was no significant change in the activated partial thromboplastin time (aPTT) clotting ($p=0.612$; Fig. 3d) or PTT clotting ($p=0.972$; Fig. 3e) times between treatment groups. There was no significant change in the liver enzyme levels (AST, $p=0.468$ and ALT, $p=0.624$) in VSV-treated versus saline-treated animals (Fig. 3f and g). The multiplex cytokine assay did not show any significant increase in cytokine levels on day 2 (data not shown).

Tissues from animals in the saline-treated and highest dose (10^9 $TCID_{50}$ or 5×10^{10} $TICD_{50}$/kg) groups were analyzed by multiplex quantitative RT-PCR for VSV nucleocapsid (N) RNA (transcripts and genome). Tissues analyzed included brain, liver, spleen, lungs, spinal cord, gonads, kidney, inguinal lymph node, and bone marrow from the femur. Day 2 samples contained the highest level of VSV-N RNA in most samples (Fig. 3). Tissues with the highest copy number per microgram of extracted RNA are listed in descending order; spleen (highest; Fig. 3h), followed by liver (Fig. 3i), lung, lymph node, kidney, gonad, and bone marrow (from femur) (data not shown). Two mice in the virus-treated group showed low positivity in brain tissue on day 2, and four mice showed positivity on day 7, suggesting that there could be viral replication in the brain (Fig. 3j). However, replication was self-limiting, and all brain samples were negative (below the level of detection) by day 21. Viremia was highest on day 2, and was negative by day 7 (Fig. 3k). Importantly, no infectious virus was recovered from brain, spinal cord, spleen, or liver at any time point even in samples with positive VSV-N RNA (data not shown).

Tissues (brain, liver, spleen, lungs, spinal cord, gonads, kidney, inguinal lymph node, bone marrow, stomach, small intestine, large intestine) harvested from mice in the saline-treated group and the 1.5×10^{10} and 5×10^{10} $TICD_{50}$/kg groups were processed for hematoxylin–eosin (H&E) staining, and stained slides were reviewed by R. Marler, a board-certified veterinary pathologist at the Mayo Clinic in Scottsdale, Arizona. No significant pathology was noted.

Efficacy and safety study in immunocompetent tumor-bearing mice

There is a possibility that robust intratumoral viral replication could increase the toxicity of systemic use of VSV. Hence, studies were also performed in immunocompetent C57BL/KaLwRij mice bearing subcutaneous syngeneic 5TGM1 plasmacytomas. Female mice were given 10^5, 10^6, 10^7, or 10^8 $TCID_{50}$ of VSV-mIFNβ-NIS intravenously. Transient weight loss was observed in all virus-treated groups (Fig. 4a). Maximum weight loss (–8.6%) was observed on day 1 in mice treated with 10^8 $TCID_{50}$, with recovery of weight by day 5. Tumor regression was dose dependent; 10^8 $TCID_{50}$-treated mice experienced the longest remission time before tumor relapse (Fig. 4b). The p values comparing the survival curves of VSV-treated mice with those of saline-treated mice are shown in Fig. 4c. The survival of mice treated with 10^7 and 10^8 $TCID_{50}$ VSV was significantly ($p=0.0008$) prolonged compared with the low-dose groups (Fig. 4c). The median survival for the saline-treated group and the groups treated with 10^5, 10^6, 10^7, or 10^8 $TCID_{50}$ of VSV-mIFNβ-NIS were 14, 19, 20, 26, and 30.5 days, respectively. The majority of mice (42 of 50) were euthanized for tumor burden, 4 for tumor ulceration of more than 50%, 2 for lethargy/moribund, and 2 were found dead. Importantly, neurotoxicity was not observed in any animals at any time. A separate cohort of mice ($n=3$ per dose level) was euthanized for correlative biodistribution studies. Quantitative RT-PCR data for VSV nucleocapsid (N) RNA performed on tumor, brain, spinal cord, spleen, liver, and ovary samples showed highest VSV-N in tumor (>10^8 copy number/μg RNA in the 10^8 $TCID_{50}$ group) on day 2. Low levels

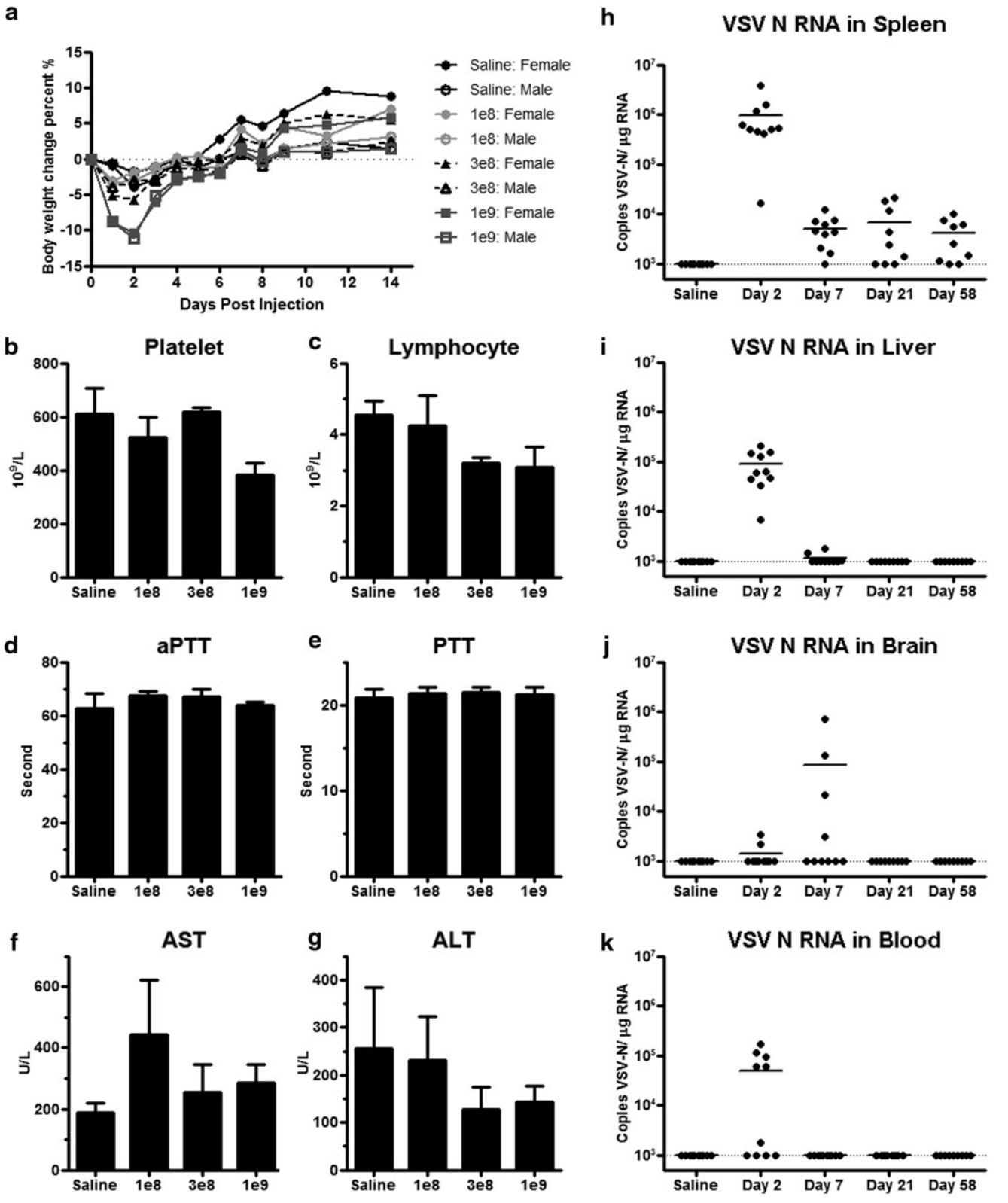

Figure 3. Toxicology and biodistribution study after intravenous administration of VSV-mIFNβ-NIS in C57BL/6 mice. **(a)** Body weight of male and female mice that received saline or 10^8, 3×10^8, or 10^9 $TCID_{50}$ of VSV. **(b)** Platelet, **(c)** lymphocyte, **(d)** aPTT, **(e)** PTT, **(f)** AST, and **(g)** ALT levels in mice on day 2 postadministration of test articles. Biodistribution of VSV-N RNA was analyzed by qRT-PCR of the **(h)** spleen, **(i)** liver, **(j)** brain, and **(k)** blood of mice given saline or 10^9 $TCID_{50}$ of VSV on day 2, 7, 21, or 58 postadministration of test articles. Limit of detection: $>10^3$ copy/μg RNA. The horizontal bars represent the mean + SEM value of the group **(b–g)** or mean value **(h–k)**. Dotted lines represent the limit of detection: 10^3 copies/μg RNA for qRT-PCR.

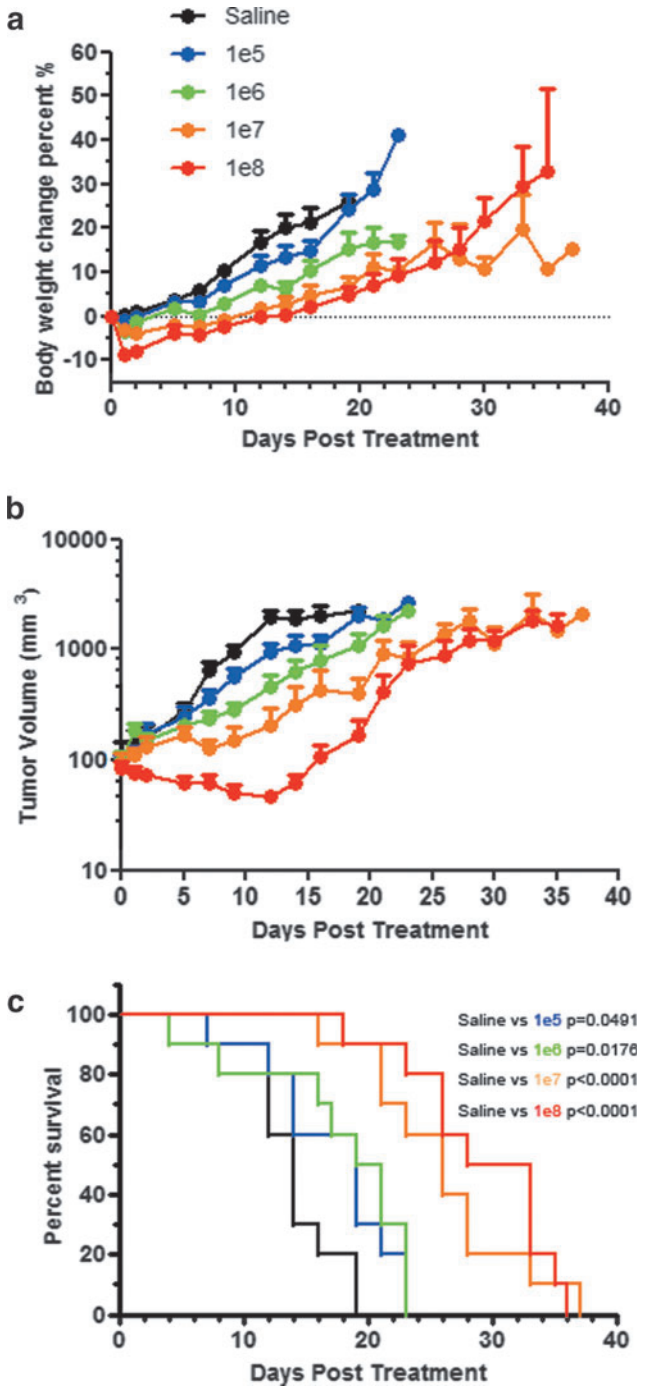

Figure 4. Efficacy study after intravenous administration of VSV-mIFNβ-NIS into immunocompetent mice with subcutaneous 5TGM1 plasmacytomas. **(a)** Change in body weight and **(b)** tumor volume, and **(c)** survival curves of mice treated with one dose of VSV at 10^5, 10^6, 10^7, or 10^8 $TCID_{50}$.

were detected in the spleen, increasing in a dose-dependent manner (Table 2). Infectious virus was recovered from the tumors (10^7 $TCID_{50}$/g tumor) in all treatment groups on day 2 (Table 2). For mice necropsied after day 2, only two mice were positive for infectious virus: 2.5×10^6 $TCID_{50}$/g tumor on day 4 and 1.9×10^3 $TCID_{50}$/g brain on day 23. Both were from the 10^6 group. It is interesting that the viral titers recovered from tumors did not correlate with treatment dose, suggesting that the virus was able to spread in this permissive tumor after initial delivery. The dose-dependent increase in mouse survival after VSV therapy (Fig. 4) could be a result of higher treatment doses eliciting a stronger antitumor T cell immune cellular response. This hypothesis remains to be tested in future studies.

No adverse events seen in tumor-bearing SCID mice treated systemically with VSV-mIFNβ-NIS

Because patients with myeloma could be immunocompromised, a SCID mouse tumor-bearing model was also used to evaluate efficacy and potential toxicity. Female SCID mice with subcutaneous human KAS6/1 myeloma xenografts were given 10^5, 10^6, 10^7, or 10^8 $TCID_{50}$ of VSV-mIFNβ-NIS intravenously. Imaging of VSV replication based on NIS reporter gene imaging, using single-photon emission computed tomography/computed tomography (SPECT/CT) on day 2, showed NIS-mediated uptake of Tc-99m pertechnetate in mice intravenously treated with VSV-mIFNβ-NIS (Fig. 5a). There was a clear correlation between the SPECT imaging data with actual dosimetric measurements of radiotracer activity in the explanted tumors (Fig. 5b). In this SCID model, tumors were effectively controlled at all dose levels tested ($p<0.0001$ by ANOVA; Fig. 5c). The survival of VSV-treated mice was significantly extended compared with saline controls, and VSV was equally effective at all dose levels tested (Fig. 5d). Quantitative RT-PCR for VSV-N showed high levels of viral transcript, indicating robust viral replication in the tumor on day 2 (Fig. 5e), and correlated well with recovery of infectious virus from the tumors (Fig. 5h). At necropsy, qRT-PCR was also performed on other tissues. Whereas qRT-PCR indicated the presence of viral RNA in the brain (Fig. 5f) and spleen of mice (Fig. 5g), infectious virus was not typically recovered in these tissues (Fig. 5h and i). Six mice, one from the saline-treated group and five from the VSV-treated groups, were euthanized between days 84 and 118 posttreatment because of hind-limb paralysis, likely due to dissemination of the myeloma into the bone marrow.[9–11] Infectious virus recovery done on the brain sample with 10^6 copies of VSV-N/μg of RNA recovered no detectable virus.

DISCUSSION

Extensive proof-of-concept and IND enabling preclinical toxicology and pharmacology studies were performed in non-tumor-bearing and tumor-bearing

Table 2. *Quantitative RT-PCR for VSV-N RNA and infectious virus recovered from major organs in mice bearing 5TGM1 tumors after treatment with one dose of 10^5, 10^6, 10^7, or 10^8 $TCID_{50}$ of VSV-mIFNβ-NIS*

	Organ	Saline	10^5 $TCID_{50}$	10^6 $TCID_{50}$	10^7 $TCID_{50}$	10^8 $TCID_{50}$
qRT-PCR for VSV-N (copy number/μg RNA)	Tumor	$<10^3$	$<10^3$	2.08×10^3	1.07×10^7	1.92×10^8
		$<10^3$	6.22×10^6	2.14×10^7	2.23×10^7	5.06×10^8
		$<10^3$	1.44×10^6	$<10^3$	$<10^3$	2.19×10^8
	Brain	$<10^3$	$<10^3$	$<10^3$	$<10^3$	$<10^3$
		$<10^3$	$<10^3$	$<10^3$	$<10^3$	$<10^3$
		$<10^3$	$<10^3$	$<10^3$	$<10^3$	$<10^3$
	Spinal cord	$<10^3$	$<10^3$	$<10^3$	1.69×10^3	$<10^3$
		$<10^3$	$<10^3$	$<10^3$	$<10^3$	4.63×10^5
		$<10^3$	$<10^3$	$<10^3$	$<10^3$	1.88×10^3
	Spleen	$<10^3$	$<10^3$	5.13×10^3	2.2×10^4	5.9×10^5
		$<10^3$	$<10^3$	1.09×10^4	1.6×10^4	7.37×10^5
		$<10^3$	$<10^3$	7.96×10^3	5.49×10^3	8.51×10^5
	Liver	$<10^3$	$<10^3$	$<10^3$	1.8×10^3	4.81×10^3
		$<10^3$	$<10^3$	$<10^3$	$<10^3$	6.15×10^3
		$<10^3$	$<10^3$	$<10^3$	1×10^3	1.27×10^4
	Ovary	$<10^3$	$<10^3$	$<10^3$	1.8×10^3	4.81×10^3
		$<10^3$	$<10^3$	$<10^3$	$<10^3$	6.15×10^3
		$<10^3$	$<10^3$	$<10^3$	1×10^3	1.27×10^4
Infectious virus recovery ($TCID_{50}$/g tissue)	Tumor	<190	3.39×10^7	<190	3.56×10^7	4.31×10^7
		<190	<190	1.9×10^5	<190	1.9×10^7
		<190	<190	<190	<190	<190
	Brain	<190	<190	<190	<190	<190
		<190	<190	<190	<190	<190
		<190	<190	<190	<190	<190
	Spleen	<190	<190	<190	1.9×10^3	<190
		<190	<190	<190	<190	<190
		<190	<190	<190	<190	<190

Note: Limit of detection for qRT-PCR: $>10^3$ and >190 for infectious virus recovery. $n=3$ mice per group.
$TCID_{50}$, 50% tissue culture infective dose; VSV-N, vesicular stomatitis virus nucleocapsid.

mice in support of clinical testing of VSV-hIFNβ-NIS as a systemic therapy in patients with cancer. Systemic administration of wild-type VSV causes lethal neurotoxicity in SCID mice.[12,13] In contrast, as shown here, no adverse clinical signs were seen when tumor-bearing SCID mice or immunocompetent C57/BL6 or C57BL/KaLwRij mice were given the laboratory-adapted Indiana strain of engineered VSV-mIFNβ-NIS at 5×10^{10} $TCID_{50}$/kg. When higher doses of virus were given, the dose-limiting toxicity with VSV-IFNβ-NIS was not neurovirulence but hepatic toxicity. The increase in AST and ALT is coupled with thrombocytopenia and lymphopenia. Elevation of transaminases was also reported as the dose-limiting toxicity associated with intravenous administration of 10^{11} $TCID_{50}$ virus into research canines.[6] Inactivated viral particles did not cause hepatic toxicity, indicating that toxicity requires virus infection. Macrophages in the liver and spleen sequester the intravenously applied virus. High copies of VSV-N were detected by qRT-PCR in the spleen and liver at 3 hr postinfusion. However, the virus did not amplify in these cells, and the VSV-N transcript levels declined over the next 2 days. No infectious viruses were recovered from the normal tissues at any dose level.

Vector-induced dose-limiting hepatotoxicity has been most studied with adenovirus (Ad).[7,14–16] Systemically administered Ads are rapidly cleared from the circulation due to sequestration by Kupffer and endothelial cells in liver sinusoids and splenic macrophages.[17] Histological analyses revealed that Kupffer cells were apoptotic (TUNEL [terminal deoxynucleotidyltransferase dUTP nick-end labeling] positive) 10–30 min after Ad infusion and necrotic within 1 hr.[8] Hepatitis could be due to infiltration of immune cells (e.g., neutrophils) in response to cytokine production and/or clearance of Ad-transduced hepatocytes by cytotoxic T cells.[18–20] Plasma levels of inflammatory cytokines (TNF-α, IFN-γ, IL-6, IL-12) increased rapidly 2–4 hr after Ad vector infusion.[7,18] By using noninfectious adenoviral particles, Wilson and colleagues showed that these inflammatory responses occur due to Ad particle interaction with host cells and do not require viral gene expression.[7] Because Ad stocks can have viral particle-to-infectious unit (VP:IU) ratios that range from 20:1 to 100:1, the MTD of Ad vectors was redefined in 1999 by the death of a patient who received Ad vector at 6×10^{11} VP/kg intravascularly and developed coagulopathy, liver damage, and multiorgan failure with prolonged high levels

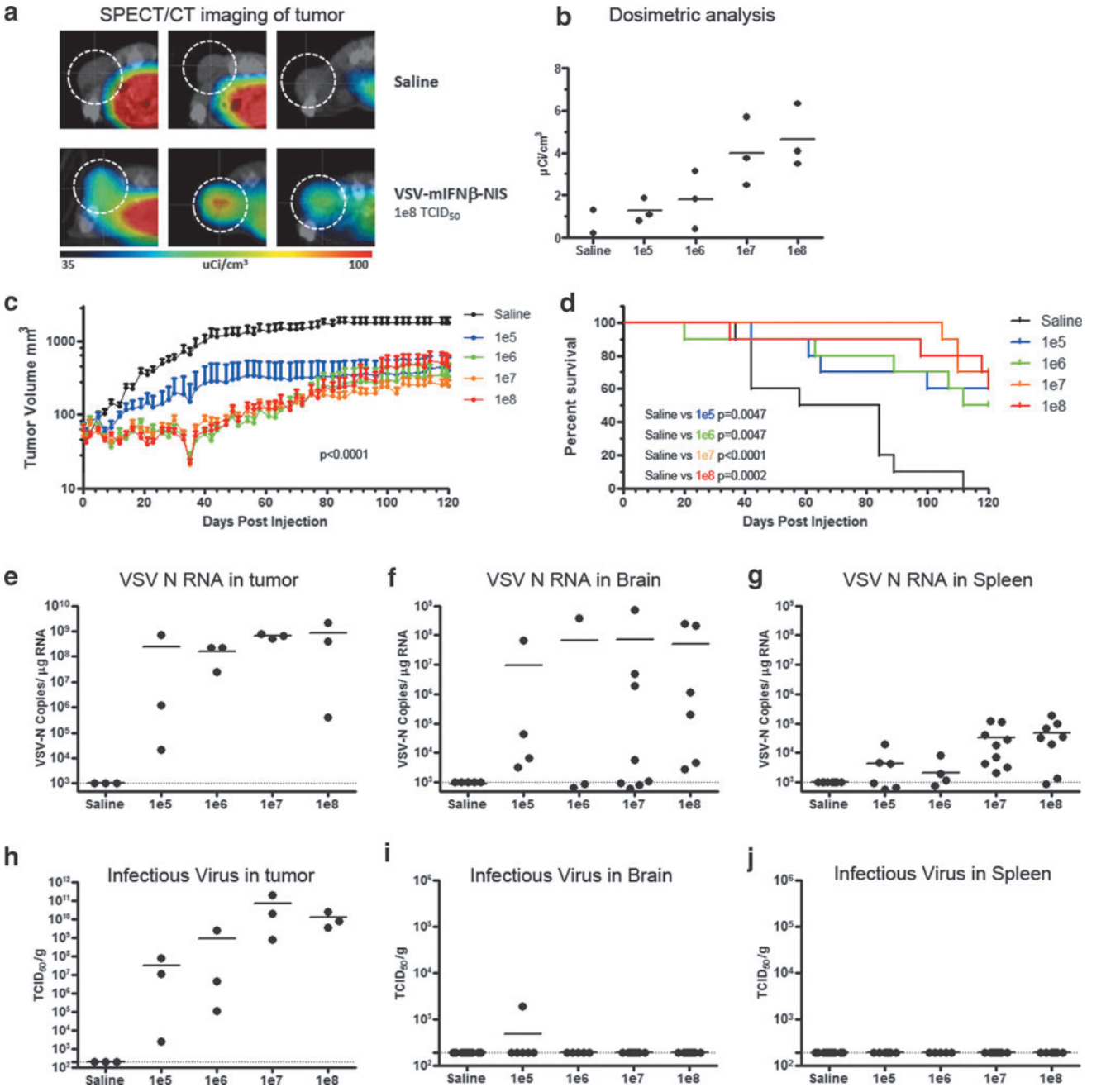

Figure 5. Efficacy study after intravenous administration of VSV-mIFN-NIS into SCID mice with human KAS6/1 myeloma xenografts. **(a)** Single-photon emission computed tomography/computed tomography (SPECT/CT) imaging showing sodium iodide symporter (NIS) expression and positive isotope uptake in tumor (circled) from mice treated with VSV but not saline, **(b)** corresponding dosimetric measurements of NIS-mediated isotope uptake, **(c)** tumor volume (mean ± SEM), and **(d)** survival curve of treated animals. Viral load was measured by qRT-PCR for VSV-N RNA or infectious virus in **(e, h)** tumor, **(f, i)** brain, and **(g, j)** spleen of animals at necropsy when the animals were euthanized for tumor burden or at the end of the study. Horizontal bars represent group medians. Dotted lines represent the limit of detection: 190 $TCID_{50}$/g for IVR, 10^3 copies/μg RNA for qRT-PCR.

of IL-6.[7] In 2000, the FDA recommended that patient doses be calculated on the basis of total number of Ad particles rather than infectious particles as "a primary toxicity of Ad vectors is mediated by an innate immune response to the viral coat proteins largely independent of the transgene expressed by the vector."

Similar to Ad particles, systemically administered VSV is rapidly sequestered by macrophages of the reticuloendothelial system. In contrast to Ad particles, VSV-induced elevation in transaminases is not due merely to the presence of large amounts of viral particles, as ultraviolet- or heat-inactivated noninfectious viral particles did not induce hepatic

toxicity. Hence, VSV dosing should remain as infectious viral rather than viral particles. The studies presented here indicate that the no observable adverse event level (NOAEL) in mice is 1.5×10^{10} $TCID_{50}$/kg, which equates to 1.5×10^{11} $TCID_{50}$ per 10-kg canine or 10^{12} $TCID_{50}$ per 70-kg human. It is currently unknown whether allometric scaling of virus dosing between species should be on the basis of body weight or surface area.[21] The generally accepted view is that it should be based on weight, which tracks with blood volume and hence with maximum circulating virus concentration after intravenous infusion. Our comparative oncology trials testing the safety of dose escalation and pharmacokinetics of VSV in companion dogs with naturally occurring cancer may shed some light on this decision. We previously reported that the severe dose-limiting hepatic toxicity occurs at 10^{11} $TCID_{50}$ and that the MTD in dogs is 10^9 $TCID_{50}$/kg, which is significantly lower than would have been predicted from the mouse studies based on body weight (1.5×10^{10} $TCID_{50}$/kg). Clearly, further studies using several species are required to shed light on allometric scaling between species for oncolytic virotherapy studies.

In summary, we have demonstrated that intravenous administration of VSV-IFNβ-NIS is well tolerated in non-tumor-bearing and tumor-bearing immunocompetent and SCID mice. No neurotoxicity was seen at the top dose tested (5×10^{10} $TCID_{50}$/kg, $\sim10^9$ $TCID_{50}$ per mouse). Instead, the dose-limiting toxicity involved transient elevation in transaminases, thrombocytopenia, and lymphopenia. The FDA has approved our IND application to proceed with clinical evaluation of the safety of intravenous VSV-mIFNβ-NIS in patients with recurrent or relapsed multiple myeloma, lymphoma, acute myeloid leukemia, and endometrial cancer. The protocol is currently under review at the Institutional Review Board of the Mayo Clinic, and we expect the trials to open for accrual in the third quarter of 2016.

MATERIALS AND METHODS

Cell culture and viruses

The 5TGM1 murine myeloma cell line (gift from B.O. Oyajobi, University of Texas Health Science Center at San Antonio, San Antonio, TX) was grown in Iscove's modified Dulbecco's medium (IMDM) supplemented with 10% fetal bovine serum (FBS), penicillin (100 U/ml), and streptomycin (100 mg/ml). Human KAS 6/1 myeloma cells (gift from D. Jelinek, Mayo Clinic, Phoenix, AZ) were grown in 10% FBS–RPMI 1640 with IL-6 (1 ng/me) and antibiotics. The cell lines tested negative for mycoplasma contamination. The construction of VSV-mIFNβ-NIS virus has been previously published.[2] The viral stock was manufactured by the Mayo Clinic Viral Vector Production Laboratory using HEK293 suspension cells under serum-free conditions. The cell culture supernatant was clarified to remove intact cells and treated with Benzonase to digest contaminating nucleic acid. This processed cell culture supernatant was then concentrated and purified by tangential flow filtration and diafiltration into a final buffer of 5% sucrose, 50 m*M* Tris-HCl, 2 m*M* $MgCl_2$ (pH 7.4). The purified virus was filtered through a final 1.5-μm (pore size) filter before final vialing. The titer of the stock (lot 2010-04, passage 4) was 6.13×10^9 $TCID_{50}$ (50% tissue culture infective dose)/ml on Vero cells. Virus was diluted in saline before use in animals. To label vesicular stomatitis virus (VSV) with DiI (1,1′-dioctadecyl-3,3,3′,3′-tetramethylindocarbocyanine perchlorate) (Cat. No. D282; Thermo Fisher Scientific, Waltham, MA), HEK293 cell was incubated with 5 μM Dil in phosphate-buffered saline (PBS) for 20 min at 37°C, before it was infected with VSV.

In vivo experiments in mice, using VSV-mIFNβ-NIS

Human myeloma cells (10^7 KAS6/1) were implanted subcutaneously in the right flank of 70 female CB17 ICR SCID mice (4–5 weeks old; Harlan Laboratories, Indianapolis, IN). 5TGM1 cells (5×10^6) were administered subcutaneously in the right flank of 65 female C57BL/KaLwRij mice (7–8 weeks old; Harlan Laboratories). Mice were randomized into treatment groups according to tumor volume when tumors measured about 5 mm in length or width. VSV-mIFNβ-NIS was administered intravenously at 10^5, 10^6, 10^7, or 10^8 $TCID_{50}$ per mouse per 100-μl injection. For the toxicology and pharmacology studies, 6- to 7-week-old (on day 0) C57BL/6 mice were used (Harlan Laboratories). On day 0, the body weight range of male and female mice was, respectively, 19.7–23.2 and 17.3–20.3 g. The average body weight for each sex was used to calculate the virus dilution needed to generate the required dose. After dosing, mice were monitored twice per day on days 1–10, due to potential neurotoxicity, and then three times per week thereafter for clinical signs. Body weights and tumor measurements were recorded three times per week until the end of the study or euthanasia of the mouse. At necropsy, tissues were collected, divided, and placed into RNA*later* (Thermo Fisher Scientific) for RT-PCR, 10% neutral-buffered formalin

for paraffin embedding and histology, embedded in Optimal Cutting Temperature (OCT) medium for immunohistochemistry, or quick frozen in liquid nitrogen for storage at ≤ –65°C for virus recovery assays. A separate cohort of mice was harvested on day 2 posttreatment for correlative assays or imaged by single-photon emission computed tomography/computed tomography (SPECT/CT) to monitor viral spread.

SPECT/CT imaging for viral spread, using sodium iodide symporter (NIS) reporter gene

Imaging was performed by the Mayo Clinic Small Animal Imaging Core with a U-SPECT-II/CT scanner (MILabs, Utrecht, The Netherlands). Animals were injected intravenously, 1 hr before imaging, with 0.5 mCi of Tc-99m sodium pertechnetate. Micro-CT image acquisition was performed in 4 min for normal resolution (169-μm^2 voxels, 640 slices) at 0.5 mA and 60 kV. The image acquisition time was approximately 20 min for SPECT (24 projections at 50 sec per bed position). Coregistration of the SPECT and CT images was performed by the application of precalibrated spatial transformation to the SPECT images to match the CT images. Data processing and quantitation of regions of interest were performed by Imanis Life Sciences (Rochester, MN), using PMOD software (Zurich, Switzerland).

Analysis for hematological, clinical chemistry, and biochemical parameters

Blood was obtained by cardiac puncture before necropsy and collected for clinical chemistry (200 μl into lithium heparin tubes; Becton Dickinson, Franklin Lakes, NJ), for complete blood count (CBC, 100 μl in EDTA tubes; Becton Dickinson), for partial thromboplastin time (PTT) and activated partial thromboplastin time (APTT) tests (sodium citrate tubes), and for RNA extraction (100 μl in RNAprotect animal blood tubes; Qiagen, Hilden, Germany); serum was also collected (600 μl in serum separator tubes; Becton Dickinson). Blood chemistry was analyzed with a Piccolo Xpress (Abaxis, Union City, CA) and CBCs were done with VetScan HM5 hematology machines (Abaxis). Clotting times were determined with a Coag Dx analyzer and IDEXX VetLab station (IDEXX, Westbrook, ME). The mouse interferon (IFN)-β multiplex cytokine assay was performed with an Invitrogen mouse cytokine magnetic 10-Plex panel kit (LMC0001M; Thermo Fisher Scientific) on a Bio-Plex 200 system (Bio-Rad, Hercules, CA).

Histology, immunofluorescence, and immunohistochemistry

Tissues embedded in OCT medium were sectioned and used for immunofluorescence staining. A rabbit antibody against VSV (M2168; Imanis Life Sciences) was used, coupled with Alexa Fluor 555-conjugated goat anti-rabbit secondary antibody (Invitrogen, A21429; Thermo Fisher Scientific). For histology and immunohistochemistry, paraffin-embedded tissues were serially sectioned, and were stained with hematoxylin and eosin (Mayo Histology Core Laboratory, Phoenix, AZ), or used for VSV immunohistochemistry using the rabbit anti-VSV antibody (diluted 1:4000) (M2168; Imanis Life Sciences).

Infectious virus recovery from tissues

Frozen samples were weighed and homogenized in 4 vol (w/v) of Opti-MEM buffer, the supernatant was clarified by centrifugation at 12,000 × g for 10 min, and 10-fold serial dilutions of samples were prepared in Opti-MEM. Aliquots (50 μl) of each dilution were placed in 96-well plates containing Vero cells. The cytopathic effects (CPEs) were recorded on day 3, and calculation for $TCID_{50}$ titer was performed as previously described.[22]

RNA extraction and q-PCR analysis

RNA from various sources were extracted, using standard kits according to the manufacturers' instructions: RNeasy Plus universal kit for tissues (73404; Qiagen) and RNeasy protect animal blood kit (73224; Qiagen). Quantitative reverse transcription-PCR was performed according to the manufacturer's instructions (LightCycler 480 RNA master hydrolysis; Roche, Indianapolis, IN) on the Roche LightCycler 480 real-time PCR thermocycler as previously described.[23]

Statistical analysis

The GraphPad Prism 5.0 program was used for data handling, analysis, and graphic representation. Kaplan–Meier survival curves were plotted and survival data were analyzed by log rank test. A Student t test or analysis of variance was used as indicated.

ACKNOWLEDGMENTS

This work was funded by the NIH/NCI (R01CA175795), the Mayo Clinic NCI-designated Comprehensive Cancer Center, a Mayo Comprehensive Cancer Center Support Grant (P30 CA015083), Mayo Clinic SPORE in Myeloma (P50CA186781), the Al and Mary Agnes McQuinn, Dorothea Berggren Charitable Foundation, and the

Mayo Foundation. The authors thank Marshall Behrens for veterinary help and acknowledge the work of the Mayo Clinic Viral Vector Production Laboratory in producing, purifying, and characterizing the VSV-mIFNβ-NIS virus, in particular Kirsten Langfield, Sharon Stephan, Deborah Melder, Henry Walker, and Gennett Pike.

AUTHOR DISCLOSURE

S.J.R., M.J.F., S.N., and K.-W.P., and the Mayo Clinic have a financial conflict of interest related to this research. This conflict is being managed by the Mayo Clinic Conflict of Interest Review Board in compliance with Mayo Clinic Conflict of Interest policies.

REFERENCES

1. Hastie E, Grdzelishvili VZ. Vesicular stomatitis virus as a flexible platform for oncolytic virotherapy against cancer. J Gen Virol 2012;93: 2529–25245.
2. Naik S, Nace R, Federspiel MJ, et al. Curative one-shot systemic virotherapy in murine myeloma. Leukemia 2012;26:1870–1878.
3. Bailey K, Kirk A, Naik S, et al. Mathematical model for radial expansion and conflation of intratumoral infectious centers predicts curative oncolytic virotherapy parameters. PLoS One 2013; 8:e73759.
4. Naik S, Nace R, Barber GN, et al. Potent systemic therapy of multiple myeloma utilizing oncolytic vesicular stomatitis virus coding for interferon-β. Cancer Gene Ther 2012;19:443–450.
5. Miller A, Nace R, Ayala-Breton CC, et al. Perfusion pressure is a critical determinant of the intratumoral extravasation of oncolytic viruses. Mol Ther 2016;24:306–317.
6. LeBlanc AK, Naik S, Galyon GD, et al. Safety studies on intravenous administration of oncolytic recombinant vesicular stomatitis virus in purpose-bred beagle dogs. Hum Gene Ther Clin Dev 2013;24:174–181.
7. Schnell MA, Zhang Y, Tazelaar J, et al. Activation of innate immunity in nonhuman primates following intraportal administration of adenoviral vectors. Mol Ther 2001;3:708–722.
8. Manickan E, Smith JS, Tian J, et al. Rapid Kupffer cell death after intravenous injection of adenovirus vectors. Mol Ther 2006;13:108–117.
9. Liu C, Russell SJ, Peng KW. Systemic therapy of disseminated myeloma in passively immunized mice using measles virus-infected cell carriers. Mol Ther 2010;18:1155–1164.
10. Huang YW, Richardson JA, Tong AW, et al. Disseminated growth of a human multiple myeloma cell line in mice with severe combined immunodeficiency disease. Cancer Res 1993;53:1392–1396.
11. Roschke V, Hausner P, Kopantzev E, et al. Disseminated growth of murine plasmacytoma: similarities to multiple myeloma. Cancer Res 1998;58: 535–541.
12. Hastie E, Cataldi M, Marriott I, et al. Understanding and altering cell tropism of vesicular stomatitis virus. Virus Res 2013;176:16–32.
13. Kelly EJ, Nace R, Barber GN, et al. Attenuation of vesicular stomatitis virus encephalitis through microRNA targeting. J Virol 2010;84:1550–1562.
14. Alemany R, Curiel DT. CAR-binding ablation does not change biodistribution and toxicity of adenoviral vectors. Gene Ther 2001;8:1347–1353.
15. Varnavski AN, Calcedo R, Bove M, et al. Evaluation of toxicity from high-dose systemic administration of recombinant adenovirus vector in vector-naive and pre-immunized mice. Gene Ther 2005;12:427–436.
16. Shayakhmetov DM, Di Paolo NC, Mossman KL. Recognition of virus infection and innate host responses to viral gene therapy vectors. Mol Ther 2010;18:1422–1429.
17. Alemany R, Suzuki K, Curiel DT. Blood clearance rates of adenovirus type 5 in mice. J Gen Virol 2000;81:2605–2609.
18. Lieber A, He CY, Meuse L, et al. The role of Kupffer cell activation and viral gene expression in early liver toxicity after infusion of recombinant adenovirus vectors. J Virol 1997;71:8798–8807.
19. Engler H, Machemer T, Philopena J, et al. Acute hepatotoxicity of oncolytic adenoviruses in mouse models is associated with expression of wild-type E1a and induction of TNF-α. Virology 2004;328:52–61.
20. Koizumi N, Yamaguchi T, Kawabata K, et al. Fiber-modified adenovirus vectors decrease liver toxicity through reduced IL-6 production. J Immunol 2007; 178:1767–1773.
21. Althaus CL. Of mice, macaques and men: scaling of virus dynamics and immune responses. Front Microbiol 2015;6:355.
22. Hadac EM, Peng KW, Nakamura T, et al. Re-engineering paramyxovirus tropism. Virology 2004; 329:217–225.
23. Jenks N, Myers R, Greiner SM, et al. Safety studies on intrahepatic or intratumoral injection of oncolytic vesicular stomatitis virus expressing interferon-β in rodents and nonhuman primates. Hum Gene Ther 2010;21:451–462.

Received for publication July 21, 2016;
accepted after revision August 4, 2016.

Published online: August 17, 2016.